Vibrational transition spectra of H_2^+ in a strong magnetic field*

Hu Shi-Lin(胡师林)[a)b)] and Shi Ting-Yun(史庭云)[a)†]

[a)] State Key Laboratory of Magnetic Resonance and Atomic and Molecular Physics, Wuhan Institute of Physics and Mathematics, Chinese Academy of Sciences, Wuhan 430071, China

[b)] University of Chinese Academy of Sciences, Beijing 100049, China

(Received 27 February 2013; revised manuscript received 2 April 2013)

Vibrational transition spectra of H_2^+ in an ultra-strong magnetic field are determined. The validity of Born–Oppenheimer approximation is analyzed based on one-center method and B-spline basis sets. It is shown that Born–Oppenheimer approximation is reliable for the investigation on the ground state and low excited states of H_2^+ subjected to the strong magnetic field. Furthermore, it is found that the vibrational transition spectra from $1\sigma_g$, $1\pi_u$, and $1\delta_g$ states lie in infrared, visible, and ultraviolet ranges with increasing magnetic field strength.

Keywords: B-spline basis, one-center method, Born–Oppenheimer approximation, vibrational transition spectra

PACS: 31.15.A–, 33.15.–e, 33.20.Tp **DOI:** 10.1088/1674-1056/22/9/093101

1. Introduction

The behaviors of molecules in the presence of a strong magnetic field have attracted a great deal of attention in the past several decades,[1,2] since ultra-strong magnetic fields were discovered in the vicinity of white dwarf stars and neutron stars in the 1970s.[3,4] Moreover, the binding energy of molecule–field systems becomes larger for stronger magnetic fields, and the potential well is deep enough to support some bound states. As a result, some peculiar molecular systems that cannot exist in the zero-field case could be present in sufficiently strong magnetic fileds, such as hydrogen chains,[5] H_4^{3+},[6] and Li_2^{5+}.[7]

The hydrogen molecular ion is the simplest molecular system, which is a good testing ground for investigating electronic properties of molecular systems in strong magnetic fields. Significant efforts have been devoted to the theoretical investigation of the hydrogen molecular ion in strong magnetic fields. Calculation of the binding energy of H_2^+ up to approximately 10^{10} G was performed,[8] in which the wave function is constructed by the orbitals of hydrogen atom in the magnetic field. A semi-analytical technique employs the wave function in terms of double power series to investigate H_2^+ subjected to a strong parallel magnetic field.[9] Although it is applied to investigate the ground state and the excited states of H_2^+ in weak magnetic fields, it provides a benchmark due to its high accuracy. A variational calculation was developed for H_2^+ in magnetic fields using a unique trial function,[10,11] but several parameters need to be optimized to obtain the minimum energy. One two-dimensional pseudospectral approach in spheroidal coordinates was proposed to study H_2^+ with a field strength smaller than $\gamma = 10$ a.u., and overcome a long-standing problem of the equilibrium distance for $1\sigma_u$ state in 1.0×10^6 T magnetic field.[12] Another Lagrange-mesh approach in spheroidal coordinates was put forward to study the ground state and excited states of H_2^+ in the strong magnetic field with high accuracy for aligned case.[13] However, the above methods need to handle complex multi-center integrals and it is difficult to include nuclear motion in spheroidal coordinates. Shortly afterward, an accurate one-center method has been advanced for the study of H_2^+ in the strong magnetic field based on B-spline basis sets, and the results could rival those obtained from multi-center calculations.[14,15] Recently, B-spline basis sets have been combined with spheroidal coordinates to obtain good results for H_2^+ under magnetic fields.[16]

However, all of the above-mentioned methods are based on Born–Oppenheimer (BO) approximation. It is well known that the binding energy becomes larger with the increase of magnetic field, and the nuclei approach each other, so the vibrational motion becomes drastic. Schmelcher *et al.*[17,18] have introduced screened BO approximation to better handle the separation of the electronic and nuclear motion in the presence of magnetic field, but no quantitative results were given. Shortly afterward, Lai *et al.*[19] and Vincke *et al.*[13] doubted the applicability of BO approximation in the strong magnetic field. In addition, harmonic approximation has been widely used to investigate vibrational energy of the ground electronic state.[10,20,21] Natural questions thus arise. Is BO approximation valid for the ground state and low excited states of H_2^+ in the super-strong magnetic field? What range are the vibrational transition spectra for the ground state and excited electronic states of H_2^+ in?

The purpose of this paper is to extend one piece of our

*Project Supported by the National Basic Research Program of China (Grant No. 2010CB832803).

†Corresponding author. E-mail: tyshi@wipm.ac.cn

© 2013 Chinese Physical Society and IOP Publishing Ltd

previous work[15] to examine the range of the validity for BO approximation in strong magnetic fields and determine the vibrational transition spectra. As is well known, it is time-consuming to study H_2^+ without BO approximation, and the BO approximation and adiabatic approximation can offer a lower bound and a upper bound to the true energy of the molecule–field system, respectively. Consequently, we perform calculations for H_2^+ in an ultra-strong magnetic field with the above approximations to test BO approximation with one-center method and B-spline basis sets, since it is convenient to take into account nuclear motion with one-center approach,[22] and the cusps can be properly approximated by B-splines.[15]

In the following sections, we will proceed as follows. In Section 2, we briefly describe the BO approximation solutions and adiabatic approximation solutions in the magnetic field. In Section 3, we present the results and discussions. In Section 4, we summarize our conclusions. Atomic units are used through this work.

2. Numerical methods

The nonrelativistic Hamiltonian of a hydrogen molecular ion in the presence of a magnetic field is expressed as[20]

$$H = \frac{1}{m_{\rm p}}\left[\left(\boldsymbol{p}_1 - \frac{\boldsymbol{A}_1}{c}\right)^2 + (\boldsymbol{p}_2 - \frac{\boldsymbol{A}_2}{c})^2\right] + \frac{(\boldsymbol{p}+\boldsymbol{A}/c)^2}{2} - \frac{1}{|\boldsymbol{r}-\boldsymbol{R}_1|} - \frac{1}{|\boldsymbol{r}-\boldsymbol{R}_2|} + \frac{1}{|\boldsymbol{R}_1-\boldsymbol{R}_2|}, \quad (1)$$

where the subscripts 1 and 2 denote the protons, and $m_{\rm p} = 1836.096$ a.u. is the proton mass. $\boldsymbol{p}$, $\boldsymbol{A}$, and $\boldsymbol{r}$ are the momentum operator, vector potential, and the position of electrons, respectively. In the following, we employ the symmetric gauge for the vector potential $\boldsymbol{A} = \frac{1}{2}\boldsymbol{B}\times\boldsymbol{r}$.

Assuming that the origin of the spherical coordinates is at the midway between the nuclei, we adopt Lasen's approach for the first term in Eq. (1), neglecting the kinetic energy of the center-of-mass motion and the field-dependent terms.[20] The Schrödinger equation of the hydrogen molecular ion in the magnetic field along the molecular axis is given by

$$H\Psi(\boldsymbol{R},\boldsymbol{r}) = E\Psi(\boldsymbol{R},\boldsymbol{r}), \quad (2)$$

where the total wave function is expanded as

$$\Psi(\boldsymbol{R},\boldsymbol{r}) = \sum_j F_j(\boldsymbol{R})\varphi_j(\boldsymbol{R},\boldsymbol{r}). \quad (3)$$

Within BO approximation, the Hamiltonian is

$$H = -\frac{1}{m_{\rm p}}\frac{\partial^2}{\partial R^2} + H_{\rm BO} = -\frac{1}{m_{\rm p}}\frac{\partial^2}{\partial R^2} - \frac{1}{2}\nabla^2 - \frac{1}{|\boldsymbol{r}-\boldsymbol{R}/2|} - \frac{1}{|\boldsymbol{r}+\boldsymbol{R}/2|} + \frac{1}{R} + \frac{1}{2}\gamma L_z + \frac{1}{8}\gamma^2 r^2(1-\xi^2), \quad (4)$$

and

$$\frac{1}{|\boldsymbol{r}\pm\boldsymbol{R}/2|} = \sum_{\lambda=0}^{\infty}(\pm)^\lambda \frac{r_<^\lambda}{r_>^{\lambda+1}} P_\lambda(\xi), \quad (5)$$

where $\boldsymbol{R}$ is the internuclear separation, r is the position of the electron, and $\xi = \cos\theta$ (θ is the angle between $\boldsymbol{r}$ and $\boldsymbol{R}$). $r_<$ ($r_>$) represents $\min(r,R/2)$ ($\max(r,R/2)$) and $\mathrm{P}_l(\xi)$ are the Legendre polynomials. $\gamma = B/B_0$ denotes the magnetic field strength, and B_0=2.35×10^5 T. The sketch map of H_2^+ in the magnetic field is shown in Fig. 1. Since the internuclear distance is regarded as a fixed parameter, the total wave function is written as

$$\Psi(\boldsymbol{R},\boldsymbol{r}) = F(\boldsymbol{R})\varphi(\boldsymbol{R},\boldsymbol{r}). \quad (6)$$

Both the electronic wave function and nuclear wave function are expanded by B-splines as

$$\varphi(R,r,\xi,\phi) = \sum_{\alpha\beta}\frac{1}{\sqrt{2\pi}}C_{\alpha\beta}(R)B_\alpha^{k_r}(R,r)(1-\xi^2)^{|m|/2} \times \left[B_\beta^{k_\xi}(\xi) + \pi B_{N_{\xi+1-\beta}}^{k_\xi}(\xi)\right]\mathrm{e}^{\mathrm{i}m\phi}, \quad (7)$$

and

$$F(R) = \sum_\mu C_\mu B_\mu^{k_R}(R), \quad (8)$$

where $k_{\rm r} = 9$ and $k_\xi = 11$ indicate the orders of radial and angular B-splines,[23–26] π denotes the parity parameter, and $(1-\xi^2)^{|m|/2}$ describes the asymptotic behavior of wave function properly in angular direction. $k_{\rm r}-2$ knots are employed at the nuclear position to speed up convergence, and the other knots are distributed exponentially.[15,23] In contrast to the angular knot distribution in Refs. [15] and [27], the angular knots are distributed in sine-like sequence in the present work,[23] since more knots are distributed around ±1 to cope with cusps. The matrix size of electronic part is $\frac{1}{2}N_{\rm r}\times N_\xi$. k_R=7 is the order of $B_\mu^{k_R}$, and the knot distribution is in equidistant sequence. In the practical calculations, the maximum radius $r = 30$ a.u., and the truncated radius $R_{\rm max}$ is 4–6 times equilibrium distance.

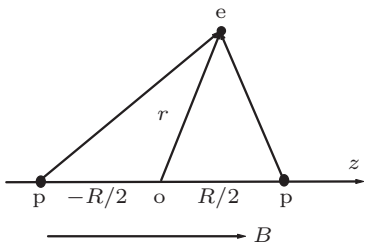


Fig. 1. Sketch map of H_2^+ in the magnetic field along the z axis.

Multiplying Eq. (2) by $\varphi(R,r,\xi,\phi)$ from left, we obtain the following equation:[28]

$$\left[-\frac{1}{m_{\rm p}}\frac{\partial^2}{\partial R^2}+\langle\varphi(R,r,\xi,\phi)|H_{\rm BO}|\varphi(R,r,\xi,\phi)\rangle\right]F(R) = EF(R). \quad (9)$$

Within the adiabatic approximation, the Hamiltonian is written as

$$\begin{aligned} H &= -\frac{1}{m_{\rm p}}\frac{\partial^2}{\partial R^2}+H_{\rm AD} \\ &= -\frac{1}{m_{\rm p}}\frac{\partial^2}{\partial R^2}-\frac{1}{2}\left(1+\frac{1}{2m_{\rm p}}\right)\nabla^2-\frac{1}{|\boldsymbol{r}-\boldsymbol{R}/2|} \\ &\quad -\frac{1}{|\boldsymbol{r}+\boldsymbol{R}/2|}+\frac{1}{R}+\frac{1}{2}\gamma L_z+\frac{1}{8}\gamma^2 r^2(1-\xi^2). \end{aligned} \quad (10)$$

Multiplying Eq. (2) by $\varphi(R,r,\xi,\phi)$ from left, we arrive at the following formula:[28]

$$\left[-\frac{1}{m_{\rm p}}\frac{\partial^2}{\partial R^2}+\langle\varphi(R,r,\xi,\phi)|H_{\rm AD}| \times\varphi(R,r,\xi,\phi)\rangle+Q(R)\right]F(R)=EF(R), \quad (11)$$

where the adiabatic correction is

$$Q(R)=-\frac{1}{m_{\rm p}}\langle\varphi(R,r,\xi,\phi)|\frac{\partial^2}{\partial R^2}|\varphi(R,r,\xi,\phi)\rangle.$$

3. Results and discussion

In all of the tables, $E_{\rm BO}$ and $E_{\rm AD}$ indicate the energies calculated within the BO approximation and the adiabatic approximation, respectively. The ΔE denotes the difference between $E_{\rm BO}$ and $E_{\rm AD}$, and $\Delta E_n = E_n - E_0$ is the difference in vibrational energy between the vibrationally excited state n and the vibrationally ground state. The N_r and N_ξ denote the number for B-splines expansion of electronic radial wave function and angular wave function, respectively. We use 194 B-splines to expand nuclear wave function. Table 1 lists the energies evaluated within BO approximation and adiabatic approximation. Compared with those in Ref. [29], our results obtained within the BO approximation and the adiabatic approximation have 7 and 5 significant digits, respectively. The $Q(R)$ in Eq. (11) has five significant digits in practical calculations, so the present results under adiabatic approximation have low accuracy. In Ref. [29], the Runge–Kutta method has been combined with Adams–Moulton numerical methodology to investigate properties of the ground electronic state, and the energies reach an accuracy of typically 9 decimal places.

Table 1. Comparison of the eigenvalues obtained within the Born–Oppenheimer approximation E_ν(BO) and the adiabatic approximation E_ν(AD) for a $1\sigma_g$ state in the absence of the magnetic field.

ν	E_ν(BO)	E_ν(BO)[29]	E_ν(AD)	E_ν(AD)[29]
0	–0.5973955	–0.597395831	–0.5971777	–0.597138381
1	–0.5874077	–0.587408102	–0.5871946	–0.587153939
2	–0.5780001	–0.578000561	–0.5777912	–0.577749204
3	–0.5691534	–0.569153956	–0.5689484	–0.568904933
4	–0.5608514	–0.560852034	–0.5606498	–0.560604884
5	–0.5530808	–0.553081471	–0.5528822	–0.552835734
6	–0.5458311	–0.545831829	–0.5456352	–0.545587051
7	–0.5390946	–0.539095576	–0.5389013	–0.538851303

In Table 2, we present the energies of $1\sigma_{\rm g}$ ($m=0$, $\pi=1$) state and $1\sigma_{\rm u}$ ($m=0$, $\pi=-1$) state within BO approximation and adiabatic approximation in different magnetic fields. For $1\sigma_{\rm g}$ state, the equilibrium distance is 1.9234 a.u. and 0.1183 a.u. for $B=0$ a.u. and $B=10000$ a.u.,[15] respectively. However, the ratios $|\Delta E/E_{\rm BO}|$ are less than 0.06%. The first excited state is the $1\sigma_u$ state, and it is antibonding and unstable in the absence of a magnetic field. For $B=10000$ a.u., the present method is not applicable for big internuclear distance, so we give rough values for $B=100$ a.u. and $B=1000$ a.u., and there is one vibrational state for $B=100$ a.u. or $B=1000$ a.u. The uncertainties $|\Delta E/E_{\rm BO}|$ are less than 0.02%, since the increase of the internuclear separation leads to the decrease in the vibrational energy. Thus, BO approximation is applicable to $1\sigma_{\rm g}$ state for $B\leq 10000$ a.u and $1\sigma_{\rm u}$ state for $B\leq 1000$ a.u.

As listed in Table 2, the energies of $1\pi_{\rm u}$ ($m=-1$, $\pi=1$) and $1\delta_{\rm g}$ ($m=-2$, $\pi=1$) states obtained within the BO approximation and the adiabatic approximation for different magnetic field strengths are shown in Table 3. For $B=10000$ a.u., the equilibrium distances of $1\pi_{\rm u}$ and $1\delta_{\rm g}$ states are 0.1536 a.u and 0.1763 a.u., respectively.[15] For $1\pi_{\rm u}$ state and $1\delta_{\rm g}$ state, the ratios $|\Delta E/E_{\rm BO}|$ are bigger than those of $1\sigma_{\rm u}$ state in the same magnetic field due to the smaller internuclear separation, but they are less than 0.06%. Consequently, the BO approximation is reliable for $1\pi_{\rm u}$ and $1\delta_{\rm g}$ states in the ultra-strong magnetic field.

Table 2. The energies obtained within the Born–Oppenheimer approximation $E_{\rm BO}$ and the adiabatic approximation $E_{\rm AD}$ for $1\sigma_{\rm g}$ state and $1\sigma_{\rm u}$ state.

	B	$E_{\rm BO}$	$E_{\rm AD}$	$\lvert\Delta E\rvert$	$\lvert\Delta E/E_{\rm BO}\rvert$/%	$N_r\times N_\xi$
$1\sigma_{\rm g}$	0	−0.5973955	−0.5971777	0.0002178	0.0364	60×60
	1	−0.4680582	−0.4677828	0.0002754	0.0588	60×60
	10	2.844782	2.845828	0.001046	0.0367	80×60
	100	44.91901	44.92674	0.00773	0.0172	80×70
	1000	488.8012	488.8717	0.0705	0.0144	80×80
	10000	4977.585	4978.271	0.686	0.0137	120×100
$1\sigma_{\rm u}$	100	46.20957	46.21726	0.00769	0.0166	200×100
	1000	492.3372	492.4074	0.0702	0.0142	220×120

Table 3. Same as Table 2, but for $1\pi_u$ state and $1\delta_g$ state.

	B	E_{BO}	E_{AD}	$\|\Delta E\|$	$\|\Delta E/E_{BO}\|/\%$	$N_r \times N_\xi$
$1\pi_u$	10	3.657775	3.659323	0.001548	0.0423	80×80
	100	46.59001	46.60417	0.01416	0.0303	80×80
	1000	492.0512	492.1888	0.1376	0.0279	100×100
	10000	4983.278	4984.643	1.365	0.0274	120×100
$1\delta_g$	10	3.932337	3.934518	0.002181	0.0555	80×80
	100	47.21575	47.23661	0.02086	0.0442	80×80
	1000	493.3471	493.5526	0.2055	0.0416	100×100
	10000	4985.675	4987.721	2.046	0.0411	120×100

Since the BO approximation is valid for the ground electronic state and low-lying states of H_2^+ in the magnetic field, now we turn to vibrational spectrum of H_2^+ under the influence of the magnetic field invoking the BO approximation. Table 4 shows that the vibrational frequencies of $1\sigma_g$ state grow with increasing magnetic field due to the deeper potential energy. The binding energies of Le Guillou and Zinn-Justin(a) and Le Guillou and Zinn-Justin(b) are calculated in the framework of improved adiabatic approximation and improved static approximation, respectively. In Refs. [10], [20], [21], [30], and [31], harmonic approximation is adopted to obtain vibrational frequencies. The results of Turbiner *et al.* and Larsen are close to Le Guillou and Zinn-Justin(b), while Le Guillou and Zinn-Justin(a) agrees with our results. Moreover, the differences between Turbiner's results and the current results increase with growing magnetic field, and the relative error is 10.8% for $B = 10000$ a.u. For $B \sim$ 1–100 a.u., the vibrational transition frequencies lie in infrared, visible, and ultraviolet ranges with growing magnetic field, respectively. For $B \sim$ 100–10000 a.u., the vibrational transition frequencies are located in the ultraviolet spectrum, which has been predicted in Ref. [32].

Table 5 lists the vibrational frequencies of the $1\pi_u$ state and the $1\delta_g$ state for different magnetic field strengths. For the $1\pi_u$ state, the vibrational transition frequencies are in infrared, visible, and ultraviolet spectra for $B \sim$ 10–100 a.u., and they lie in visible and ultraviolet ranges for $B \sim$ 100–10000 a.u. For the $1\delta_g$ state, the vibrational transition frequencies are located in infrared, visible, and ultraviolet spectra for $B \sim$ 10–100 a.u., and in visible and ultraviolet ranges for $B \sim$ 100–10000 a.u.

Table 4. Vibrational transition frequencies corresponding to the $1\sigma_g$ state.

	B/a.u.	ΔE_1	ΔE_2	ΔE_3	ΔE_4
Present	0	0.00998	0.01939	0.02824	0.03654
Wille[21]		0.0108			
Present	1	0.01328	0.02589	0.03783	0.04911
Turbiner[10]		0.014			
Larsen[20]		0.014			
Le Guillou and Zinn-Justin(a)[30]		0.013			
Le Guillou and Zinn-Justin(b)[30]		0.014			
Present	10	0.03787	0.07376	0.10774	0.13982
Turbiner[10]		0.040			
Larsen[20]		0.040			
Wunner[31]		0.036			
Le Guillou and Zinn-Justin(a)[30]		0.039			
Le Guillou and Zinn-Justin(b)[30]		0.040			
Present	100	0.12339	0.23902	0.34726	0.44849
Turbiner[10]		0.132			
Larsen[20]		0.141			
Wunner[31]		0.13			
Le Guillou and Zinn-Justin(a)[30]		0.128			
Le Guillou and Zinn-Justin(b)[30]		0.132			
Present	1000	0.3588	0.6896	0.9948	1.2764
Turbiner[10]		0.390			
Larsen[20]		0.38			
Wunner[31]		0.39			
Le Guillou and Zinn-Justin(a)[30]		0.366			
Le Guillou and Zinn-Justin(b)[30]		0.388			
Present	10000	0.896	1.708	2.446	3.117
Turbiner[10]		0.993			

Table 5. Same as Table 4, but for $1\pi_u$ state and $1\delta_g$ state.

	B/a.u.	ΔE_1	ΔE_2	ΔE_3	ΔE_4
$1\pi_u$	10	0.01958	0.03827	0.05608	0.07301
	100	0.07183	0.13961	0.20348	0.26359
	1000	0.2272	0.4383	0.6344	0.8165
	10000	0.611	1.166	1.682	2.147
$1\delta_g$	10	0.01425	0.02787	0.04090	0.05332
	100	0.0544	0.10598	0.15471	0.20069
	1000	0.1789	0.3458	0.5013	0.6462
	10000	0.505	0.966	1.388	1.774

4. Conclusions

By combining the one-center method and B-splines, we have carried out calculations for the ground state and some low excited states of H_2^+ in the ultra-strong magnetic field within the BO approximation and the adiabatic approximation, and determined the vibrational transition frequency range. Our results are in reasonable agreement with other theoretical values obtained within the BO approximation and the adiabatic approximation for the field-free case. In addition, it is concluded that BO approximation is valid for the ground state and low excited states of H_2^+ in the strong magnetic field. At the same time, it is found that the vibrational energy increases with growing magnetic field, and the relative difference of vibrationally ground state energy for the $1\sigma_g$ state is less than 10.8% for the harmonic approximation. Finally, it is shown that vibrational transition frequencies of $1\sigma_g$, $1\pi_u$, and $1\delta_g$ states lie in infrared, visible, and ultraviolet ranges with the growth of magnetic field. Thus, the current results offer a useful tool to identify the observed spectra of neutron star 1E1207.4-5209.[33]

References

[1] Wang D H and Ding S L 2004 *Chin. Phys.* **13** 30

[2] Wang D H, Song X X and Ding S L 2008 *Chin. Phys. B* **17** 599

[3] Schmelcher P and Schweizer W 1998 *Atoms and Molecules in Strong External Fields* (New York: Plenum)

[4] Lai D 2001 *Rev. Mod. Phys.* **73** 629

[5] Lai D, Salpeter E E and Shapiro S L 1992 *Phys. Rev. A* **45** 4832

[6] López V J C and Turbiner A 2000 *Phys. Rev. A* **62** 022510

[7] Olivares-Pilón H, Bayer D, Turbiner A V and López Vieyra J C 2010 *J. Phys. B* **43** 065702

[8] de Melo L C, Das T K, Ferreira R C, Miranda L C M and Brandi H S 1978 *Phys. Rev. A* **18** 12

[9] Kravchenko Y P and Liberman M A 1997 *Phys. Rev. A* **55** 2701

[10] Turbiner A V and López Vieyra J C 2004 *Phys. Rev. A* **69** 053413

[11] Turbiner A V and López Vieyra J C 2006 *Phys. Rep.* **424** 309

[12] Guan X X, Li B W and Taylor K T 2003 *J. Phys. B* **36** 3569

[13] Vincke M and Baye D 2006 *J. Phys. B* **39** 2605

[14] Zhang Y X, Kang S and Shi T Y 2008 *Chin. Phys. Lett.* **25** 3946

[15] Zhang Y X, Liu Q and Shi T Y 2012 *J. Phys. B* **45** 085101

[16] Zhang Y X, Liu Q and Shi T Y 2013 *Chin. Phys. Lett.* **30** 043101

[17] Schmelcher P, Cederbaum L S and Meyer H D 1988 *Phys. Rev. A* **38** 6066

[18] Schmelcher P, Cederbaum L S and Meyer H D 1988 *J. Phys. B* **21** L445

[19] Lai D and Salpeter E E 1996 *Phys. Rev. A* **53** 152

[20] Larsen D M 1982 *Phys. Rev. A* **25** 1295

[21] Wille U 1987 *J. Phys. B* **20** L417

[22] Kempe J A and Goldman S P 1998 *J. Chem. Phys.* **108** 7679

[23] Bachau H, Cormier E, Decleva P, Hansen J E and Martín F 2001 *Rep. Prog. Phys.* **64** 1815

[24] Kang S, Liu Q, Zhong Z X, Zhang X Z and Shi T Y 2006 *Acta Phys. Sin.* **55** 3380 (in Chinese)

[25] Meng H Y, Kang S, Shi T Y and Zhan M S 2007 *Acta Phys. Sin.* **56** 3198 (in Chinese)

[26] Zhou X X, Li X Y and He Y L 2008 *Acta Phys. Sin.* **57** 116 (in Chinese)

[27] Kang S, Li J and Shi T Y 2006 *J. Phys. B* **39** 3491

[28] Carrington A, McNab I R and Montgomerie C A 1989 *J. Phys. B* **22** 3551

[29] Beckel C L, Hansen B D and Peek J M 1970 *J. Chem. Phys.* **53** 3681

[30] Le Guillou J C and Zinn-Justin J 1984 *Ann. Phys. (N.Y.)* **154** 440

[31] Wunner G, Herold H and Ruder H 1982 *Phys. Lett. A* **88** 344

[32] de Melo C P, Ferreira R, Brandi H S and Miranda L C M 1976 *Phys. Rev. Lett.* **37** 676

[33] Sanwal D, Pavlov G G, Zavlin V E and Teter M A 2002 *Astrophys. J. Lett.* **574** L61